Chin. J. Astron. Astrophys. Vol. 4 (2004), No. 1, 88–96
(http://www.chjaa.org or http://chjaa.bao.ac.cn)

Chinese Journal of
Astronomy and
Astrophysics

A Photometry Campaign for IR Geminorum in Quiescence*

Hai Fu[1], Zong-Yun Li[1], Kam-Ching Leung[2], Zhou-Sheng Zhang[3], Zi-Li Li[3] and C. Martin Gaskell[2]

[1] Department of Astronomy, Nanjing University, Nanjing 210093; zyli@nju.edu.cn
[2] Department of Physics and Astronomy, University of Nebraska, Lincoln NE 68588-0111, USA
[3] Yunnan Observatory, Kunming 650011

Received 2003 May 22; accepted 2003 June 16

Abstract We report a V band photometry of the SU UMa star IR Gem at quiescence in January 2002. The observations were made with two telescopes spaced $\sim 160°$ apart in longitude. Several photometric modulations have been found. One gives a period of 98.50(13) min, exactly equal to the orbital period determined spectroscopically. Two others occasionally strengthen and seem to be positive and negative superhumps with periods of 103.6(4) and 95.4(4) min, 5.2% longer and 3.1% shorter than the orbital period, respectively. A signal at ~ 0.6 c/d in the power spectrum is roughly consistent with the expected period of nodal precession of the disk. There is a puzzling peak at 0.21(3) c/d corresponding to the ~ 4.3 d sine wave seen in the raw light curve. We suspect it to be a beat frequency between the frequencies of apsidal and nodal precessions of the disk. Quasi-periodic cycles with amplitudes 0.15–0.6 mag can be seen in the light curve. The mechanism underlying this modulation is not clear.

Key words: accretion, accretion disks — binaries: close — novae, cataclysmic variables — stars: dwarf nova — stars: individual (IR Geminorum)

1 INTRODUCTION

SU UMa stars, which comprise a subclass of dwarf novae, were identified with their distinctive superoutbursts and accompanying superhump phenomena (see Warner 1995 §3.6 for a comprehensive review). IR Gem was discovered to be an SU UMa star by Szkody, Shafter & Cowley (1984, hereafter SSC), who conducted the first systematic investigation on this object, determined a characteristic superhump period of 102 min from photometric data collected during a superoutburst, and detected a 101 min modulation (with amplitude 0.4–0.6 mag in V band) at quiescence, which was interpreted to be an orbital effect of irradiation of the secondary. Furthermore, based on the small K1 value (30 ± 4 km s^{-1}) and the strong "orbital"

* Supported by the National Natural Science Foundation of China.

modulation, the authors presumed that IR Gem consisted of a massive white dwarf and possibly a heated degenerate secondary. However, the paper left a confusing problem that the "orbital" modulation of 101 min is slightly but not negligibly discrepant with the 98.5 min periodicity obtained from radial velocity curve of Hα line.

More recent work confirmed the 98.5 min spectroscopic period in phase-depended EW variations of Hα (Làzaro, Martìnez-Pais & Arèvalo 1991) and UV resonance lines (Woods et al. 1992), as well as radial velocity curve of Hβ and Hγ (Feinswog, Szkody & Garnavich 1988). Superhumps with a mean period of $\sim$102 min, 3.7% in excess of the orbital period, were registered during its 1991 March superoutburst (Kato 2001), further confirming its identity as an SU UMa star. Nevertheless, the photometric modulation in quiescent state behaves erratically: sometimes it seems to be almost disappeared (Feinswog, Szkody & Garnavich 1988), but then it reappeared with a larger amplitude (Szkody et al. 1989). Szkody et al. (1989) suggested that the modulation amplitude might depend on outburst phase since the former light curve was obtained just before an outburst while the latter, 8 days after an outburst (the average outburst period of IR Gem is 21 days. Note also, the 101 min modulation SSC described was observed 5 days before an outburst). However, previous photometry was not adequate to address this issue. In this paper we report a time-resolved photometry of IR Gem starting 3 days after an outburst maximum and lasting over 6 days. Our observations trace the changing course of the "orbital" modulation and thus are helpful for understanding its erratic behavior.

2 OBSERVATIONS

We carried out almost continuous photometric observations of IR Gem in quiescence for a period of 6.5 days (from 2002 January 19 to 25, UT) at Yunnan Observatory (YNO) in China and the Behlen Observatory (BO), University of Nebraska, USA. The time difference between the two sites is approximately 11 hours. The Yunnan Observatory images were collected using a TEK1024 CCD camera attached to the Cassegrain focus of a 1.0 m reflector, while the Behlen Observatory images were taken with a 0.75 m reflector equipped with an ST-9E CCD camera and focal reducer. A standard V filter was used on both telescopes. Exposure times were set long enough to guarantee good signal-to-noise ratios. A total of 1783 useful frames were processed as described in Gao et al. (1999). A journal of observations is given in Table 1.

Table 1 Journal of Observations

Date(UT) (Year 2002)	Run	HJD Start −2,452,000	HJD End −2,452,000	Exposure (s)	Number of Images	Site
Jan 19	1	293.9968	294.3678	60	301	YNO
Jan 20	2	294.6058	294.8554	120	79	BO
Jan 20	3	295.1441	295.1877	150	22	YNO
Jan 21	4	295.6023	295.9368	120	170	BO
Jan 21	5	296.0031	296.3705	150	177	YNO
Jan 22	6	296.6682	296.9334	180	92	BO
Jan 22	7	297.0482	297.3506	100	180	YNO
Jan 23	8	297.5411	297.8559	180	83	BO
Jan 23	9	298.0335	298.1482	100	21	YNO
Jan 24	10	298.5554	298.9554	150	189	BO
Jan 24	11	299.0104	299.2494	100	134	YNO
Jan 25	12	299.5399	299.8733	150	152	BO
Jan 25	13	300.0064	300.3018	100	183	YNO

Differential magnitudes of IR Gem were obtained using two secondary photometric standards, stars 5 and 6 on the finding chart of Misselt (1996), as the comparison star (C) and check star (K), respectively. From the method suggested by Howell, Jitchell & Warnock (1988), we estimate the standard deviation of the differential magnitudes of V-C at 0.02–0.03 mag for the YNO data and 0.03–0.04 mag for the Behlen data.

3 RESULTS AND ANALYSIS

The unpublished light curve provided by the AAVSO (Mattei 2002) indicates that IR Gem has recovered from a normal outburst that had reached its maximum just three days before our observations. All of the photometric data are shown in Fig. 1. Since the data were collected in the two hemispheres, the observations mostly lasted 16–21 hours (with a gap of 1 or 2 hours) every day and so provide a good database for period analysis. Figure 1 also shows the best linear fit to the light curve. From this fit we estimate that the rate of decline was 0.135(3) mag/d.

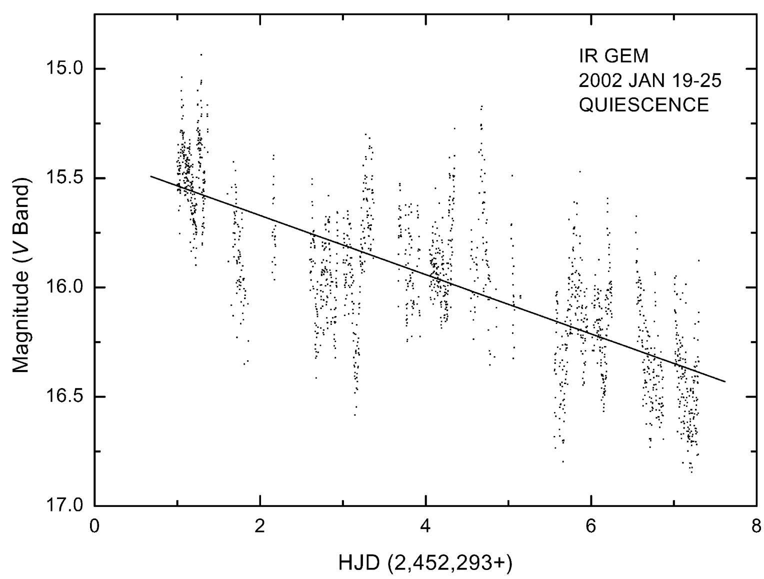

Fig. 1 Full light curve of the observations. The ordinate presents the estimated magnitudes based on a comparison star of *V* magnitude 13.761(30). The solid line shows the best linear fit to the data.

3.1 Signals Near the Orbital Frequency

In the complicated power spectrum of the star (see Fig. 4), there are only small spikes at 14.62(2) and 15.17(2) c/d around the orbital frequency. In order to study the periodicities near the orbital frequency, one should remove the longer-period components. Following Larionov, Lyuty & Zaitseva (2001), we smoothed the light curve using the method of a sliding window with a width Δ:

$$m_i' = -2.5\log\left(\frac{1}{\sum p_j}\sum_{j=1}^{k} p_j \cdot 10^{-0.4m_j}\right), \tag{1}$$

where k is the number of data points within interval $[t_i - \Delta, t_i + \Delta]$, and the weight of the jth point is determined as

$$p_j = \exp\left[-(\delta t_j/\Delta)^2\right], \tag{2}$$

where δt_j is the time span from the jth point to the center of the window. We then subtracted the smoothed curve from the raw light curve to produce residuals. The optimal value of the smoothing interval Δ was chosen to be 0.05 d by trials: it gives the most effective suppression of the lower frequency components and the highest signal-to-noise ratio in the vicinity of the orbital frequency.

In the CLEAN spectrum (Roberts, Lehar & Dreher 1987) of the residuals, a prominent peak became visible at 14.61(2) c/d, i.e., a period of 98.56(13) min, which exactly equals the spectroscopically determined orbital period (SSC; Feinswog, Szkody & Garnavich 1988). The folded light curve at this frequency shows a sinusoidal profile with a peak-to-trough amplitude of ~ 0.08 mag (Fig. 2).

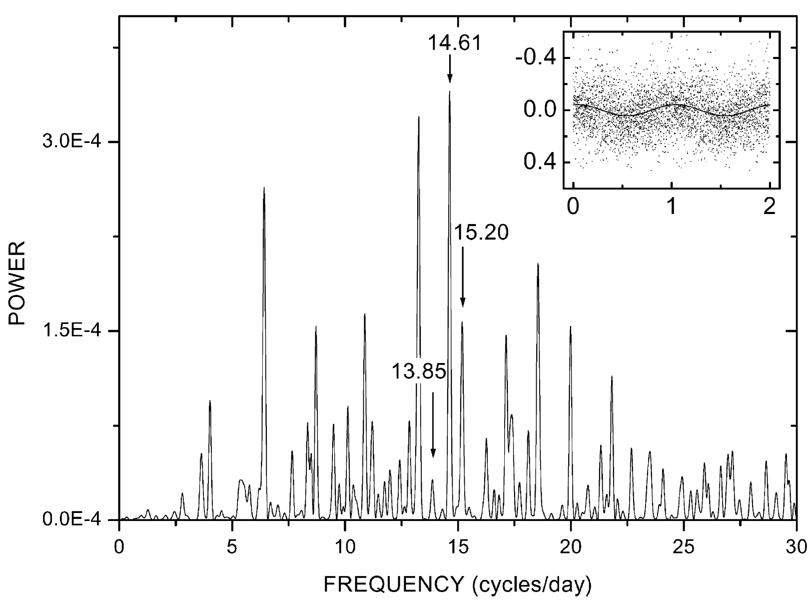

Fig. 2 CLEAN spectrum of the residuals (see text). The most prominent peak corresponds to a period of 98.56(13) min. *inset*, where the dependence of the V magnitude on the phase of the 98.56 min period for the residuals, with least squares fit of a sine wave, is shown by the solid line. Phase zero is arbitrarily chosen to be the beginning of observations.

Our good temporal coverage enables us to do period analysis on 2-day long segments of the residuals separately. The results are presented in Fig. 3. Only one peak at 13.90(5) c/d occurs between 10 and 16 c/d in the CLEAN spectrum of Part I (runs 1 to 4); the most prominent feature appears at 15.10(6) c/d for Part II (runs 5 to 8); and for Part III (the last 5 runs), a remarkable peak occurs at 14.58(6) c/d. Note that the periods 103.6(4) and 95.4(4) min, corresponding to the frequencies 13.90 and 15.10 c/d, are 5.2% longer and 3.1% shorter than the orbital period of 98.5 min, respectively. Also shown in Fig. 3 are waveforms of the segments folded at frequencies 13.90, 15.10 and 14.61 c/d, respectively.

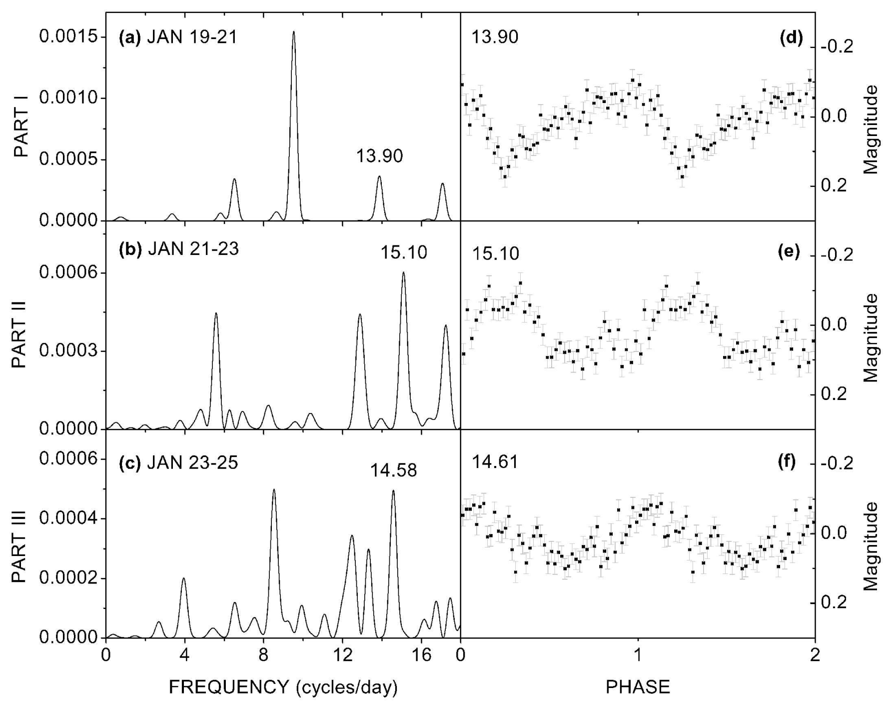

Fig. 3 Period analysis of separate 2-day long segments of the residuals after subtraction of lower frequency components. (a), (b) and (c), CLEAN spectra of each segments (labels are centered over the peaks). Dates are shown on the upper left of each frame. (d), (e) and (f), Wave forms of each segments. Folding frequencies are labeled on the upper left of each frame.

In order to check whether uncorrelated noise could be responsible for the presence of these signals, we shuffled each segment randomly, and then computed the power spectrum for each random configuration. In 100 simulations, no other peak between 13 and 16 c/d exceeded the ones found in the observed time series. The periodicities will be discussed further in Sect. 4.

3.1.1 The Coherence of the Periods

We estimate the phase of a signal from a least-squares fit of a fixed frequency sine function for individual runs (Henney & Harvey 2002). Runs 3 & 9 are excluded for their scarcity of data. Each of the time series is fitted at periods 103.6, 95.4 and 98.5 min independently, then the best one was chosen under the criteria of χ^2 and amplitude. In all our cases, the lowest χ^2 value always brings the largest amplitude.

The results listed in Table 2 clearly show that the periods 103.6 and 95.4 min, which showed up in Part I and Part II respectively, are highly coherent, while the 98.5 min period seems only marginally coherent. Perhaps the somewhat disordered pattern is due to the faintness of the

DN or/and the damping of the modulation during the last two days (This fact could also be appreciated from their large fitting errors.).

Table 2 Phase Values for Individual Runs

Run	Period (min)	Phase[a]	Error[b]
1	103.6	0.058	0.027
2	103.6	–0.058	0.043
4	103.6	0.035	0.029
5	103.6	–0.035	0.063
6	95.4	0.024	0.039
7	95.4	0.053	0.024
8	95.4	–0.077	0.032
10	98.5	0.020	0.038
11	98.5	–0.090	0.063
12	98.5	0.119	0.070
13	98.5	–0.048	0.056

[a] Displayed relative to the mean phase of separate groups as divided by small skips.
[b] Fitting errors at a confidence level of 95%.

3.2 Variation on a 4–5 Day Timescale

We computed the CLEAN spectrum of the complete set of de-trended data (Fig. 4) which had been generated by subtracting the linear decline from the original light curve. The highest peak in the spectrum appears at frequency 0.21(3) c/d. Although the time series is short for determining a period of 4–5 d, the sinusoidal variation with a timescale of $\sim$ 4.3 d and a full amplitude of $\sim$ 0.24 mag is quite evident in the raw light curve (Fig. 1).

3.3 Apparent Quasi-Periodic Cycles

In the light curve, there are prominent large-amplitude (0.15–0.6 mag) cycles that occurred in a quasi-periodic fashion. Those cycles are responsible for the high peak stands at frequency 3.66(2) c/d as well as the lower peaks in its vicinity. After subtracting a best fit sinusoidal at 0.21 c/d from the de-trended light curve, the residuals were folded at 3.66(2) c/d and show a sine waveform with a full amplitude of 0.19(8) mag. The mechanism underlying this modulation is, however, not clear. A similar cycle with an amplitude of 0.5 mag can also be seen in the light curve of Feinswog, Szkody & Garnavich (1988).

4 DISCUSSION

We believe the modulation at 14.62 c/d is certainly an orbital effect. It has an amplitude of $\sim$ 0.08 mag and a period exactly equal to that deduced from spectroscopy. Unfortunately, the ephemeris available is not accurate enough to check at what phase the modulation is a maximum, and so we can not recognize definitely whether it is due to a hot spot or just heating of the secondary. However, we tend to attribute it to the latter because of its sinusoidal waveform. Since it has a small amplitude, this modulation does not suffer from the energetic problem posed by SSC where the 0.5 mag modulation observed in quiescence needs an X-ray flux 10 times higher than the observed level if it is a heating effect.

We suggest that the mechanism underlying the 13.90 c/d modulation appearing in the first three days is similar to that of a late superhump (Hessman et al. 1992). Its light source should mainly be the hot spot where the inflow stream strikes the disk, because the mean profile of the modulation (Fig. 3d) shows a slow rise followed by a steep decline. This is a typical feature of hot spot modulations. The longer period (103.6 min) variation could easily be explained as beating between the orbital motion and the apsidal precession of an eccentric disk. It is reminiscent of the 0.5 mag 101 min modulation caught by SSC. We suspect that it is also produced by the hot spot. Its larger amplitude simply indicates a larger $\dot{M}2$.

In our second segment, a sinusoidal modulation with a period of $\sim$ 95.4 min dominates the power spectrum. This could be explained by an episodically tilting disk (Harvey et al. 1998). When disk tilting occurs, the mass transfer stream overshoots its rim, so we can no longer see the hot spot modulation. The disk's node immediately begins retrograde precession in the orbital plane; the negative superhump (the 95-min modulation) is thus produced.

According to the nodal precession model, the negative superhump period of 95.4 min and the orbital period of 98.5 min demand that the tilted disk be in retrograde precession at a rate of 2.08(35) d per cycle. We indeed find that a spike appears at $\sim$ 0.55 c/d in the CLEAN spectrum for the complete set (Fig. 4), while a more prominent peak at $\sim$ 0.6 c/d is present in the runs 4 to 13 (the figure has not been shown, for saving space). These features provide independent evidence for the validity of the model.

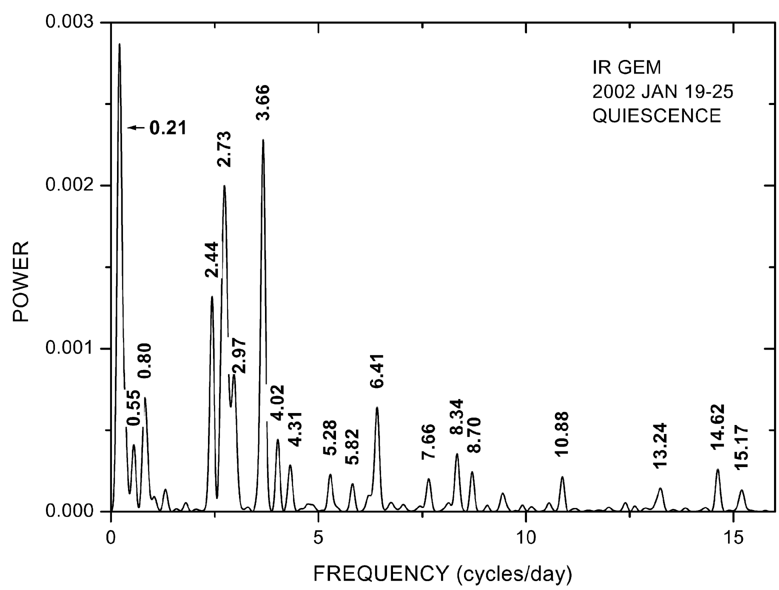

Fig. 4 CLEAN spectrum of the complete set of the de-trend time series, showing a strong signal at 0.21 c/d. The complicated pattern suggests multi-periods. Spikes at 14.62 and 15.17 c/d can also be seen.

If apsidal and nodal precessions operate simultaneously in the disk of IR Gem, the modulation at 0.21(3) c/d in Fig. 4 or the $\sim$ 4.3 d sinusoidal variations visible in Fig. 1 can be tentatively understood as beating between the two modes. We suspect the spikes at $\sim$ 0.55 and $\sim$ 0.8 c/d to be signatures of precession of the disk. Correlations between the intensity variations of orbital modulation, positive and negative superhumps, and phase of the 4.3 d cycle could support this suggestion to some extent. Unfortunately, our observations are not adequate for us to address this problem.

Although it is rare to observe superhumps in quiescent states, there have been other well-documented examples. AL Com showed persistent superhumps as well as orbital humps at quiescence (Patterson et al. 1996). EG Cnc sustained its late superhumps for at least 90 d after the 1996 superoutburst (Patterson et al. 1998). ER UMa, which has an extremely short superoutburst cycle and essentially no quiescence, also showed superhumps in minima of outbursts (Gao et al. 1999). More recently, Woudt & Warner (2001) found V359 Cen showing superhumps with a period of 112 min and V630 Sgr to be an eclipsing permanent superhumper with evidence of disk precession in both the complete set of raw light curves and the Fourier amplitude spectrum.

5 SUMMARY

The main conclusions we draw are as follows:

(1) The modulation at 14.62(2) c/d gives an orbital period of 98.50(13) min, exactly equal to that obtained spectroscopically. We tentatively attribute this to heating of the secondary.

(2) The signal at 13.90(5) c/d appearing mainly on the first three days corresponds to a period of 103.6(4) min, 5.2% longer than the orbital period. The modulation shows a slow rise followed by a steep decline in its mean waveform. We suggest that it might be a signature of the apsidal precession of an eccentric disk.

(3) The feature at 15.10(6) c/d strengthening on January 21– 23 represents a periodic modulation of 95.4(4) min, which is 3.1% shorter than the orbital period. We invoke nodal precession of a tilted disk to explain it. A signal at ~ 0.6 c/d is roughly consistent with the expected period of nodal precession.

(4) The peak at 0.21(3) c/d corresponding to the ~ 4.3 d sine wave seen in the raw light curve is puzzling. We suspect that it may be the result of beating between apsidal and nodal precession frequencies.

(5) Quasi-periodic cycles with an amplitudes of 0.15–0.6 mag can be seen in both the raw light curve and in the power spectrum. The time scales of the variations were drifting from ~ 0.2 to ~ 0.4 d. The mechanism underlying this modulation is not clear.

Some signals in the power spectrum have not been identified.

Our observations show that the behavior of IR Gem in quiescence is unexpectedly complicated and that further observations will be invaluable. Clearly, for IR Gem, quiescence is more interesting than outbursts.

Acknowledgements We would like to thank Professor Peisheng Chen of Yunnan Observatory and Professor Edward G. Schmidt of Behlen Observatory for scheduling the observations. We are grateful for financial support from the National Natural Science Foundation of China (through grants 10173005 and 10010120074) and the Department of Physics and Astronomy at the University of Nebraska.

References

Feinswog L., Szkody P., Garnavich P., 1988, AJ, 96, 1702
Gao W., Li Z., Wu X., Zhang Z., Li Y., 1999, ApJ, 527, L55
Harvey D. A., Skillman D. R., Kemp J. et al., 1998, ApJ, 493, L105
Henney C. J., Harvey J. W., 2002, Solar Phys., 207, 199
Hessman F. V., Mantel K. -H., Barwig H., Schoembs R., 1992, A&A, 263, 147
Howell S. B., Jitchell K. J., Warnock A., III., 1988, AJ, 95, 247
Kato T., 2001, IBVS, 5122, 1
Larionov V., Lyuty V. M., Zaitseva G. V., 2001, A&A, 378, 837
Làzaro C., Martìnez-Pais I. G., Arèvalo M. J., 1991, AJ, 101, 196
Mattei J. A., 2002, Observations from the AAVSO International Database, private communication
Misselt K. A., 1996, PASP, 108, 146
Patterson J., Augusteijn T., Harvey D. A. et al., 1996, PASP, 108, 748
Patterson J., Kemp J., Skillman D. R. et al., 1998, PASP, 110, 1290
Roberts D. H., Lehar J., Dreher J. W., 1987, AJ, 93, 968
Szkody P., Howell S. B., Mateo M., Kreidl T. J., 1989, PASP, 101, 899
Szkody P., Shafter A. W., Cowley A. P., 1984, ApJ, 282, 236 (SSC)
Warner B., 1995, Cataclysmic Variable Stars, Cambridge: Cambridge University Press
Woods J. A., Verbunt F., Collier Cameron A., Drew J. E., Piters A., 1992, MNRAS, 255, 237
Woudt P. A., Warner B., 2001, MNRAS, 328, 159